IEEE Access
Multidisciplinary | Rapid Review | Open Access Journal

Received 27 September 2023, accepted 13 October 2023, date of publication 31 October 2023, date of current version 9 November 2023.

Digital Object Identifier 10.1109/ACCESS.2023.3328910

RESEARCH ARTICLE

Design and Construction of a Solar Electric Plastic Extruder Machine Based on a Parabolic Trough Collector

JOSÉ ALONSO DENA-AGUILAR[1,2], (Member, IEEE), ARTURO DÍAZ-PONCE[3], JUAN CARLOS DELGADO-FLORES[2], ERNESTO OLVERA-GONZÁLEZ[4], NIVIA ESCALANTE-GARCÍA[4], AND VÍCTOR MANUEL VELASCO-GALLARDO[2]

[1]EPM CONAHCYT, Centro de Investigaciones en Óptica, A. C. Unidad Aguascalientes, Aguascalientes 20200, Mexico
[2]Engineering Department, Instituto Tecnológico de Pabellón de Arteaga, Tecnológico Nacional de México, Pabellón de Arteaga, Aguascalientes 20670, Mexico
[3]CONAHCYT, Centro de Investigaciones en Óptica, A. C. Unidad Aguascalientes, Aguascalientes 20200, Mexico
[4]Artificial Lighting Laboratory, Instituto Tecnológico de Pabellón de Arteaga, Tecnológico Nacional de México, Pabellón de Arteaga, Aguascalientes 20670, Mexico

Corresponding authors: Arturo Díaz-Ponce (adiaz@cio.mx) and José Alonso Dena-Aguilar (josealonso_dena@hotmail.com)

This work was supported in part by the CONAHCYT-Mexico under Grant EPM 1086950 and Grant 270828; in part by Instituto Tecnológico de Pabellón de Arteaga, Tecnológico Nacional de México (TecNM) Campus; and in part by Instituto de Ciencia y Tecnología del Estado de Aguascalientes (INCYTEA) (before IDSCEA)-Aguascalientes under Project IA-025-2019.

ABSTRACT Plastics can be recycled by extrusion using an extruder machine that melts and transforms the material into a new product. This paper proposes the design, construction and thermal characterization of a horizontal extruder machine integrated with a parabolic trough concentrator with a one-axis solar tracking system, in which hybrid heating is performed by means of an arrangement of electrical resistances and by the concentration of direct normal irradiance. The optical simulation and the design of the proposed extruder are presented; as well as its integration with the parabolic trough concentrator. Experimental tests were performed in a real environment and the temperatures reached in three cases of heating by electrical resistance, solar radiation, and hybrid (electrical resistance plus solar radiation) were compared. The objective is to reach a temperature of 200 °C in the barrel, for which an analysis of the experimental thermal performance of the proposed extruder is presented. The heating by electrical resistances took from 77 to 95 min to reach 200 °C, while the hybrid system only took 25 to 57 min, reducing the times between 25.97 and 73.68% and, consequently, reducing the consumption of resistor current. In hybrid mode, at one point in the barrel, temperatures higher than 260 °C were reached, providing the possibility of instantly turning off some electrical resistances to save energy.

INDEX TERMS Plastic extrusion, extruder machine, parabolic trough collector, solar tracker, concentrated solar power.

I. INTRODUCTION

Waste plastics are durable and non-biodegradable materials that can be subjected to recycling processes to manufacture new products through the use of mechanical or chemical recycling technologies such as extrusion, injection molding, pyrolysis, and liquefaction, among others [1], [2]. One of the most widely used plastic polymer recycling processes today is extrusion, which is carried out in extruder machines and whose operating principle is based on melting the material previously crushed into flakes and placing it in contact with a rotating and hot endless screw that moves the material forward. Said endless screw is housed in an extrusion barrel provided with a thermal system that allows reaching sufficient temperatures to melt the plastic and make it pass through an opening until it is picked up by the extrusion

The associate editor coordinating the review of this manuscript and approving it for publication was R. K. Saket.

nozzle [3], [4], [5]. Typically, in extruder machines, electrical resistances are used as a heating system to achieve working temperatures, melt the material and extrude thermoplastics in products such as hoses [6], composite filaments [7], and pellets [8], among other applications.

On the other hand, it is well known that solar energy can be used in various applications, such as building heating, water heating, the operation of drying, dehydrating or desalination units, or electricity generation, among other applications [9], [10], [11], [12], [13], [14]. However, few studies report the use or feasibility of employing solar energy in extrusion processes. The authors of [15] propose the use of solar energy stored in a battery to power the instrumentation of extrusion equipment integrated into a 3D printer. Similarly, the authors of [16] computationally estimate the operating parameters of an extrusion process to propose the design of the extruder equipment with an integrated Fresnel solar concentrator.

There are two types of solar concentration technologies: linear and point focus. Point focus systems, such as central tower and parabolic dish systems, can reach extremely high temperatures (above 500 °C) due to their high solar concentration levels. However, these systems only focus energy on one point and require monitoring on two axes, making them more complex.

On the other hand, linear focus solar concentration technologies, like linear Fresnel and Parabolic Trough Collector (PTC) systems, are considered medium temperature (150-400°C) [17], [18].

Due to its technological maturity, the PTCs are one of the most widely used Concentrated Solar Power (CSP) technologies within industrial processes for the application of solar heating. PTCs are designed to collect and concentrate the sun's infrared heat, which can then be stored or transferred without any energy transformation. As a result, these systems boast an impressive efficiency rate of 70-80% [19]. PTCs are commonly used for solar process heat production due to their technological maturity and profitability. They are more efficient than photovoltaic systems, which only convert 10-15% of solar radiation into electricity [20].

A PTC is a system that has a parabolic collector that concentrates solar radiation in a receiver located at the linear focus of the parabola [21], [22], [23]. This concentration allows for reaching temperatures ranging between 100 and 400 °C [24], [25], which is why they have been development and implemented in various applications such as pasteurization, cooking, washing, distillation, fluid heating, and boiler preheating, among others [26], [27], [28], [29], [30]. The main disadvantage of PTCs is that they can only concentrate Direct Normal Irradiation (DNI), so they necessarily require a Solar Tracking System (STS) on one axis to achieve automatic orientation solar rays towards the receptor during the day [31]. In particular, the authors of [26] developed a PTC with a copper helical coil receiver through which water flows as a heat transfer fluid and manages to reach maximum working temperatures of 107 °C. In the work of [27], maximum temperatures of 155 °C were obtained by developing a PTC with a glass absorber tube as a receiver. Likewise, [28] presented a summary of thermal applications of solar energy with a focus on the use of PTCs in heating, cooling, and desalination processes, where PTCs can reach heat temperatures of up to 400 °C. In other papers, the authors of [29] and [30] report, respectively, the use of PTCs in concentrated solar power plants for steam generation and to preheat seawater deposited in a distillation pond within a desalination process. As observed in the literature, PTC systems have been used to carry out various low and médium-temperature applications; however, to date, no studies have been carried out on the integration and use of solar energy, through a PTC with solar tracking, in the extrusion process or thermoplastics and/or waste plastics in horizontal extrusion machines.

This paper proposes the integration of a hybrid heating system by solar and electric energy in a pilot plant of a single screw horizontal extruder. On the one hand, a PTC system with solar tracking concentrates the DNI on a linear focus where the barrel (receiver) of the machine is installed, and, on the other hand, a backup system made by an arrangement of electrical resistances provides the remaining heat necessary to reach the melting temperature of the plastics used (typically between 180 and 280 °C depending on the type of plastic to be extruded [32]). For this work, a temperature of 200 ±15 °C, the average extrusion temperature of Low-Density Polyethylene (LDPE) [33], [34], was established as the desired response variable to be achieved in the receiver.

The organization of this manuscript will be as follows: Section II presents an opto-energetic analysis of the designed PTC, in which the flow distribution in the receiver and the system acceptance angle are analyzed. In addition, the designs and characteristics of the PTC and the extruder machine are described; as well as, the design and control of the solar tracking system is presented. In Section III, the configuration of the proposed hybrid extruder machine is shown and the thermal characterization methodology used is specified. In addition, the experimental results on the temperatures reached in the receiver by the three case studies are presented: exclusive heating by means of solar energy, heating with electrical resistances, and hybrid heating. Finally, Section IV presents the conclusions of this work.

II. DESIGNS AND MATERIALS

Figure 1 shows a diagram of the total development stages of the project, i.e., the development of the PTC, the Extruder Machine (EM) and the Solar Tracking System (ST).

For the development of this project, firstly, the design and optical simulation of the parabolic trough system was carried out to determine its dimensions and the average solar concentration on the receiver. Later, the mechanical design of the PTC was elaborated in Solidworks® to plan its integration into the proposed extruder machine. In order for the PTC

to take advantage of most of the DNI throughout the day, a one-axis solar tracking system was developed, which uses a closed-loop on-off control algorithm. In order to focus on the thermal results achieved by the extruder, in this study only its component parts are shown. The following sections provide the most important details of the above-mentioned items.

A. SIMULATION AND OPTICAL ANALYSIS OF THE PTC SYSTEM

In order to define the physical parameters of the parabolic concentrator and the receiving barrel, in addition to estimating the maximum and average solar concentration and calculating the acceptance angle of the proposed system, an optical analysis was carried out in the Tonatiuh ray tracing software, which uses the Monte Carlo method to optically simulate concentrating solar systems. For the simulation the following parameters were defined: pill Box'' like a kind of Sun, with 1×10^3 W/m^2 of solar irradiance, 0.00465 maximum theta rad, 1×10^6 rays, and solar elevation angles of 82.5, 85, 87.5 and 90°.

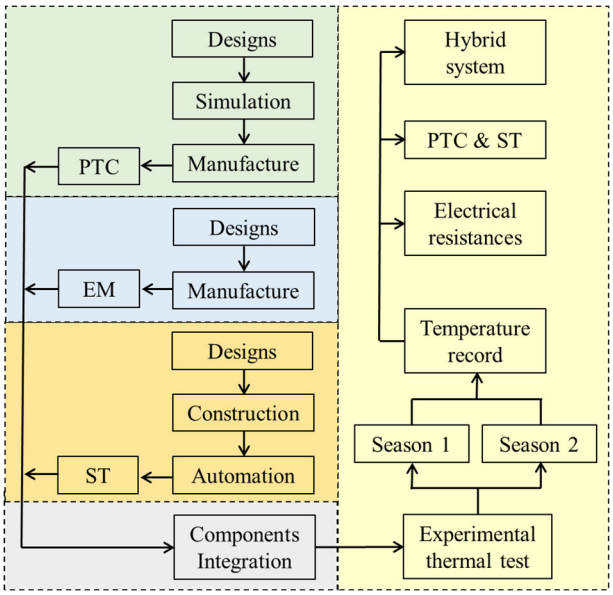

FIGURE 1. Block diagram of the project stages: PTC, extruder machine (EM) and solar tracker system (ST).

Figure 2 shows the simulation of the parabolic trough concentrator and the receiver tube based on the measurements of the proposed PTC (2000 mm straight side, 960 mm wide, and 500 mm parabolic focus). In this image it can be seen that when the incident solar radiation is perfectly perpendicular to the normal surface of the concentrator; that is, when the Solar Tracking Error (STE) is equal to 0°, all the photons that hit the surface of the reflective concentrator are redirected towards the focal point of the parabola, where it is located at the receiver (barrel) of the extruder. Note that the solar concentration is found mainly on the sides of the receiving tube since there is no concentration in the upper part and the radiation level is 1x; which is 1,000 W/m^2. The maximum solar concentration level in the receiver is up to 10.03x (10,030 W/m^2); the average solar concentration is 3.85x.

Likewise, Figure 3 shows the incident flux distribution in the receiver when there is no solar tracking error, which is completely homogeneous throughout the receiver (the x-axis corresponds to the width and the axis and length of the receiver). It was concluded that the average solar concentration is sufficient for the proposed pilot plant, so the selected measures are adequate.

After establishing and validating the physical dimensions of the PTC, an analysis of the collector optical losses caused by the STE was performed, which allowed us to analyze the impact of the solar tracking accuracy of the system. An STE of different degrees was induced in simulation to divert the incident solar radiation and analyze the behavior of the system's maximum and average solar concentration, in addition to studying the flux distribution in the receiver. It is worth mentioning that this analysis was only carried out on the axis of movement of the system and it was considered that the orientation of the PTC is north-south, so the monitoring is carried out from east to west.

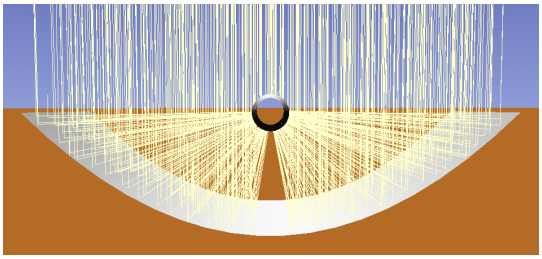

FIGURE 2. Photon flux map when the angle formed between the incident solar radiation and the surface is 90° (ideal position); that is, with a STE=0°.

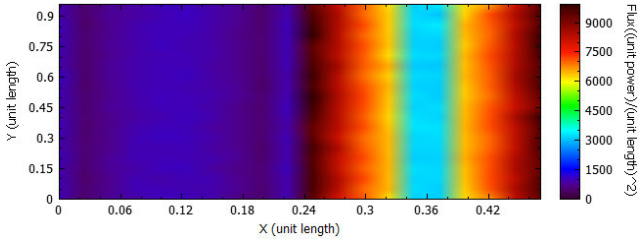

FIGURE 3. Incident flux distribution in the receiving tube with a STE=0°.

Figure 4 shows the photon map obtained with an STE of 2.5°, 5°, and 7.5°. It is observed that the concentration in the receptor tends to go up on the right side and down on the left side, this depends on the sign of the STE. Note that in 5° and 7.5°, the STE is already so large that most of the photons do not hit the receiver, resulting in a decrease in the average solar concentration of the system.

Table 1 details the levels of solar concentration in the receiver, where it can be seen that even when 0° <STE<5°, the maximum solar concentration is higher than with STE=0°, but the flow distribution is low, which generates

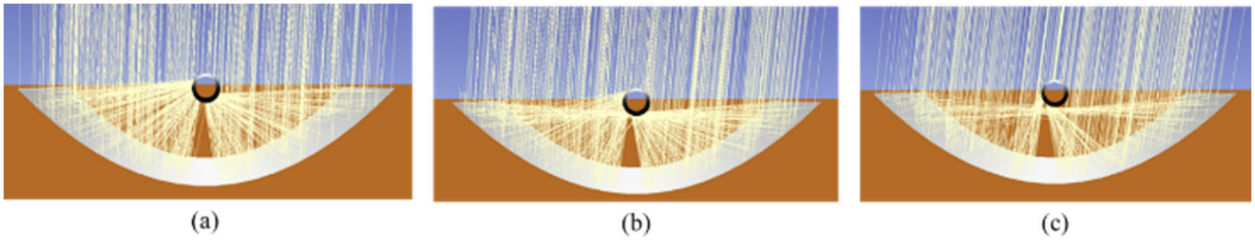

FIGURE 4. Photon flux map when the angle of incident radiation and the surface normal is: a) 87.5° (STE=2.5°), b) 85° (STE=5°), and c) 82.5° (STE=7.5°).

TABLE 1. Theoretical concentration levels achieved with different STE.

STE	Average concentration (W/m^2)	Maximum concentration (W/m^2)
0°	3,847	10,018
2.5°	3,841	13,549
5°	3,262	17,294
7.5°	1,488	7,191

thermal stress in the receiving tube. On the other hand, the average solar concentration decreases as the STE increases and, consequently, the energy efficiency also decreases.

Finally, to know the required precision of the PTC solar tracking system, the acceptance angle (θ_a) in the tracking axis was determined by means of a simulation; that is, the angle when the incident average flow losses are of the order of 2° [35].

Figure 5 shows the relationship between the STE and the average solar concentration, in which it is observed that the θ_a obtained was ±4.2°, that is, even when the STE=4.2° the average solar flux is guaranteed to be 98%. After this angle, the average concentration drops dramatically. Therefore, it is concluded that, in order to maintain acceptable optical efficiency, the solar tracking system is required to have a precision greater than |4.2°|, which represents a wide tracking tolerance. Based on this, the actuators, solar sensors, controller, control algorithm, and mechanical transmission system, among others, were selected for the solar tracking system.

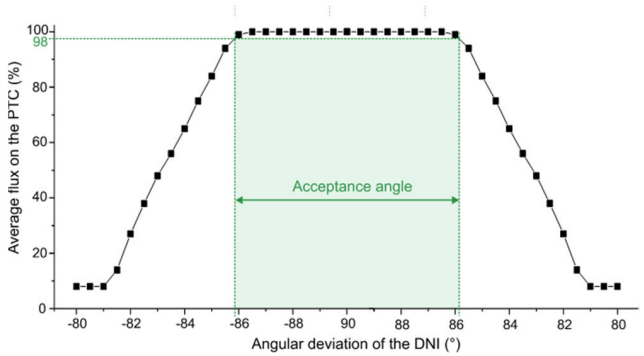

FIGURE 5. Changes in the average incident flow due to changes in the angular deviation of the DNI.

B. MECHANICAL DESIGN OF THE PTC SYSTEM

After carrying out the optical simulation, the mechanical simulation of the extruder elements was carried out, the most important elements being the parabolic collector and the horizontal extruder machine. The PTC was designed to sit on a commercial carbon steel frame that allows it to maintain its parabolic geometry and remain balanced via a barrel-matched floating support system. The PTC rotates through a mechanical transmission system made up of a Direct Current (DC) motor, a gear motor, and a winch system and cable. The linear focus of the parabola remains constant at a 500 mm focal radius, the place where the barrel (receiver) of the extruder was installed and where the sun's rays are concentrated during the day. Figure 6 shows the design of the PTC and its components: (A) the reflective optical element (parabolic collector) consisting of a 2000 mm long and 960 mm wide natural aluminum sheet with a mirror finish, 18-gauge; (B) the floating support system that is made up of 2 vertical guides with circular terminals adaptable to the barrel, which are integrated into the frame by means of fastening screws, (C) the receiver (barrel), (D) the frame, which is made up of 3 1/4" steel arches (2 arches of 2 m on a straight side and 1 arch of 1 m on a straight side) and 4 1/8 × 3/4" steel screed

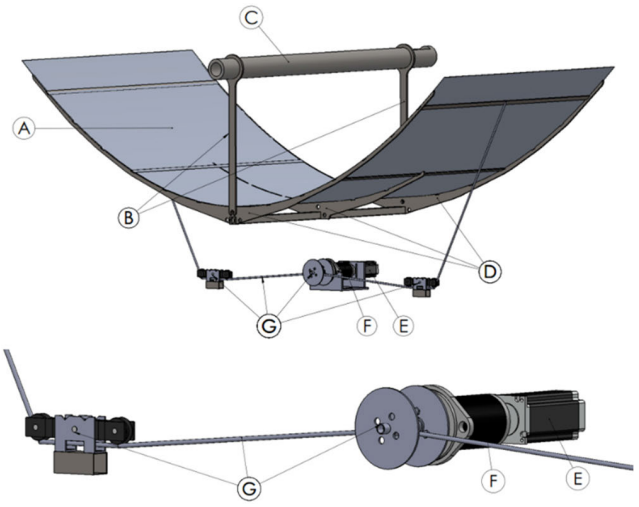

FIGURE 6. Isometric design of the reflecting dish: A) reflective optical element (dish), B) floating vertical supports, C) receiver (barrel), D) frame, E) gear motor, F) DC motor, and G) winch system.

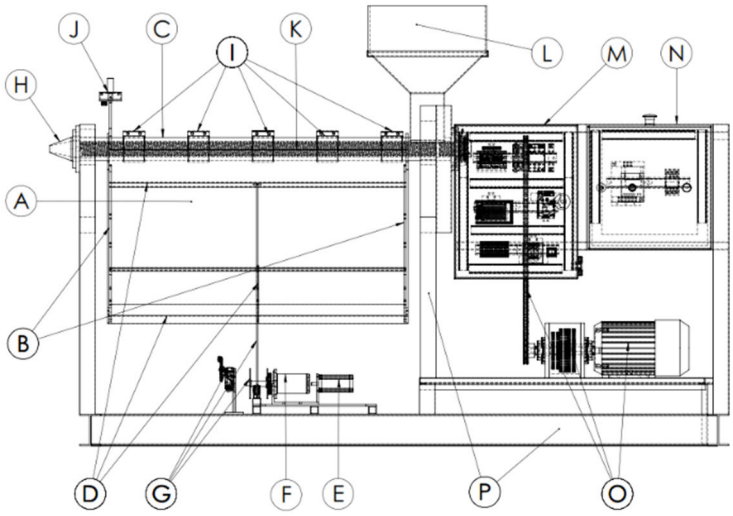

FIGURE 7. Technical drawing of the extruder machine: A) PTC, B) floating vertical supports, C) barrel (receiver), D) frame, E) gear motor, F) DC motor, G) winch system, H) extruder mouth, I) resistors electrical, J) solar sensor, K) spindle, L) feed hopper, M) solar tracking panel, N) 220V electrical control panel, O) power transmission equipment (AC motor, gearbox, chain) and P) support structure.

TABLE 2. Approximate cost of the PTC.

PIECES	ELEMENT	COST (USD)
1	Reflective optical element	$156.0
1	Frame	$191.29
1	Floating support system	$18.69
1	Mechanical transmission system	$128.88
	Total	$494.87

secondary support elements. The design also contemplates a mechanical transmission system made up of: (E) a 50:1 gear ratio gear motor, (F) a NEMA 23 model OK57H18112A 4.2A, 3Nm motor, and (G) a winch system with 3/32'' steel cable and sliding double-packed trolley-type guides. Table 2 describes the main elements of the raw material cost used in the construction of the PTC, without considering labor costs or other expenses. The total approximate cost of the developed PTC was $494.87 USD.

C. MECHANICAL DESIGN OF THE HORIZONTAL EXTRUDER MACHINE

Starting from the design of the previous PTC, a single screw horizontal extruder machine pilot plant was designed, which has a support structure with a geometry capable of integrating the PTC with the solar tracking system and other components, as shown in the technical drawing in Figure 7.

The screw, the extruder mouth, the feeding Hopper, and the barrel constitute the extrusion module. For this study, the barrel works as the receiving device of the present work, which is kept at a fixed point due to the architecture of the extruder. The barrel consists of a cylindrical perforated steel bar of 8630 steel with 1200 mm long and with internal and external diameters of 50 and 75 mm, respectively (other elements of the extrusion module are not described). The electrical control panel and power transmission equipment modules are used to control the rotational speed of the spindle (modules not described). The sun tracking control panel is used to control the automatic movement of the PTC by means of the sun sensor in relation to the apparent movement of the Sun during the day. A set of 5 electrical resistances connected in parallel constitutes the electrical heating system. Each band-type resistor is 500W at 220V and 3'' in diameter with an integrated type k thermocouple. The integral operating principle of the machine is of the conventional type, where the raw material in the form of flakes is fed through the feeding hopper to come into contact with the spindle housed inside the barrel, which is heated and rotated to allow the material melts and passes through an extruder mouth, adopting a new geometry. The resistors are connected in series and placed equidistantly on the barrel. In hybrid mode, the resistors are used in conjunction with the PTC with solar tracking to provide the working heat required to melt the raw material.

D. DESIGN AND CONTROL OF THE SOLAR TRACKING SYSTEM

The solar tracking control was carried out using an on-off control algorithm with tracking Hysteresis (H) shown in Figure 8. This control is fed back by a solar sensor based on the voltage difference generated by an electronic arrangement with 2 Light Depending Resistors (LDR_1 and LDR_2); which is $R_{dif} = LDR_1 - LDR_2$. The control system error (e) is calculated by $e = Ref - R_{dif}$, where Ref is the desired reference, in this case $Ref = 0$. With the value of e, the control algorithm is capable of sending the control signal (u) to activate the actuators of the system by means of an analogue driver.

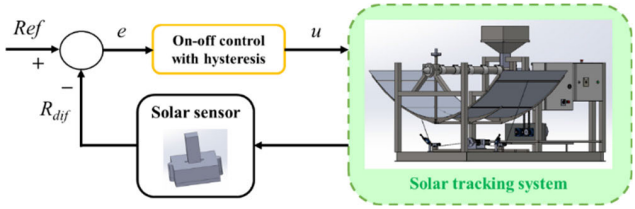

FIGURE 8. Block diagram of the solar tracking control system.

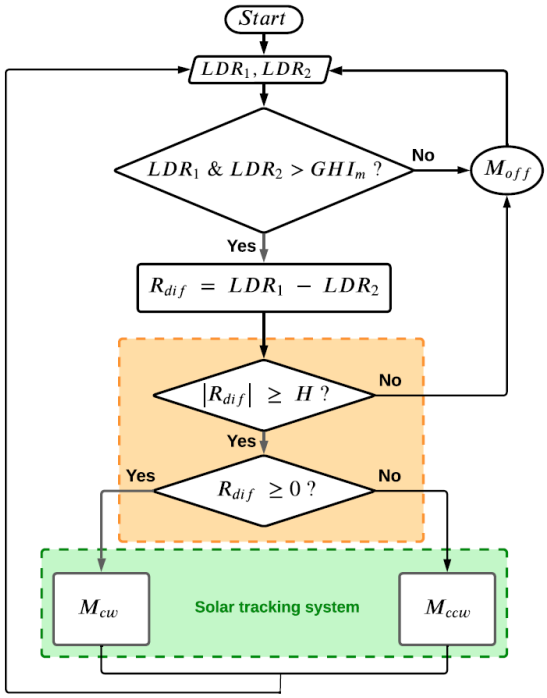

FIGURE 9. Closed-loop control system flowchart.

The PTC DC motor rotates to the west when the counterclockwise rotation is activated (M_{CW}), otherwise, turn east counterclockwise (M_{CCW}).

In the same way, Figure 9 presents the flowchart of the tracking algorithm, which executes the following processes:

1. The voltage generated by the electronic arrangement is obtained with the LDR.
2. Said signals are digitized to obtain LDR_1 and LDR_2 and are compared with the digital value produced by the Minimum Instantaneous Global Horizontal Irradiance (GHI_m) required to perform sun tracking. In the case study, it was experimentally established GHI_m=3V, which is the voltage that is generated when the global radiation is at least 500 W/m^2. This allows, in case of cloudiness or darkness, the solar tracker to remain off (M_{off}), which avoids energy waste. It should be mentioned that the photoresistors generate a value of 1024 adc for a radiation of 1,000 W/m^2 and about 0 adc when in total darkness. In short, when LDR_1 and LDR_2 are greater than GHI_m, the tracker starts its routine; otherwise, it remains immobile until the radiation is the minimum allowable.
3. The difference between the values produced by the photoresistors is calculated, R_{dif}=LDR_1−LDR_2.
4. When $|R_{dif}|$ is greater than or equal to H, the tracker is disoriented and needs to correct its position. On the contrary, when $|R_{dif}|e = Ref - Rdif$ is less than H, the tracker is positioned perpendicular to the Sun's rays with the allowable margin of error and does not require relocation, therefore the DC motor remains off. It is worth mentioning that, due to the nature of photoresistors and diffuse solar radiation, it is very rare that R_{dif} is equal to zero during sun tracking. The hysteresis was set experimentally to 2V, value that occurs when the tracking error is approximately 2°, which is within the acceptance angle of the designed system (see Section II-A), so we ensure that the efficiency of the PTC is greater than 98%.
5. Finally, to determine the direction of rotation required by the PTC; when $R_{dif} \geq \mathbf{0}$, the motor rotates M_{CW} to the west, otherwise turn M_{CCW} to the east.

The solar sensor was developed by placing the photoresistors (LDR_1 and LDR_2) on an electronic printed circuit board installed inside a base (casing) designed with an obelisk-type divider, which provides a shading on one or the other sensor according to the apparent position of the Sun during the day. In Figure 10, the manufactured solar sensor is presented. The holes in the white casing act as windows that allow solar radiation to fall directly on the photoresistors. The voltage difference generated with the electronic arrangement of the resistors allows to command the direction of rotation of the DC motor of the PTC to concentrate the maximum solar radiation on the receiver.

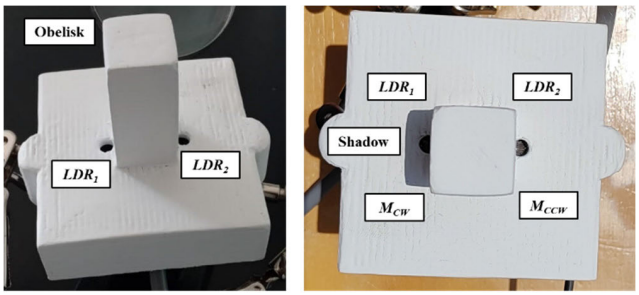

FIGURE 10. Solar sensor: a) windows and obelisk top view, and b) under the Sun view.

Figure 11 shows the monitoring and control board of the solar tracking system, with the Raspberry Pi 3B card being the main control element due to its processing speed, which is why the general program was carried out in Python. An Arduino Mega 2560 board is used as a data acquisition card.

In order for the user to easily manipulate the proposed extruder, a Human-Machine Interface (HMI) was developed through a 7'' Nextion touch screen, in which it is possible to

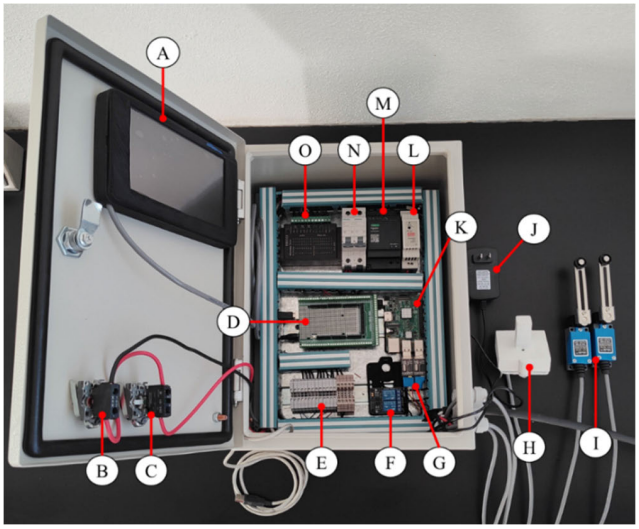

FIGURE 11. Solar tracking system monitoring and control panel: A) HMI, B) pilot light, C) On-off selector, D) Arduino Mega 2560 card with shield, E) 5V-12V DIN terminals, F) SDR-05V relays, G) CH340G module, H) solar sensor, I) limit switch ME-8108, J) 5V-1A Arduino and 5V-3A RPi power supplies, K) RPi 3B board, L) 100-240VAC 5V 2.4 power supply A, M) 100-240AC 24V 2.5A power supply, N) 5SL6106 and 5SL6104 switches, and O) TB6600 driver.

monitor the variables of interest and command system operation (manual or automatic mode) and make configurations. In automatic mode, the PTC follows the apparent position of the Sun during the day; in manual mode, the PTC can rotate on its tracking axis to M_{CW} and M_{CCW} according to the user's decision and in this way, it can be used to maintain or place or remove elements of the system.

Figure 12 shows the HMI, which was also designed in Python using the Tkinter graphics library, on the main screen it can be seen: (a) the position of the PTC calculated with the pulses of the DC stepper motor, (b) the values of the photoresistors and their differential voltage R_{dif}, and (c) the required GHI_m for tracking to take place and (d) the current value of the tracking hysteresis H.

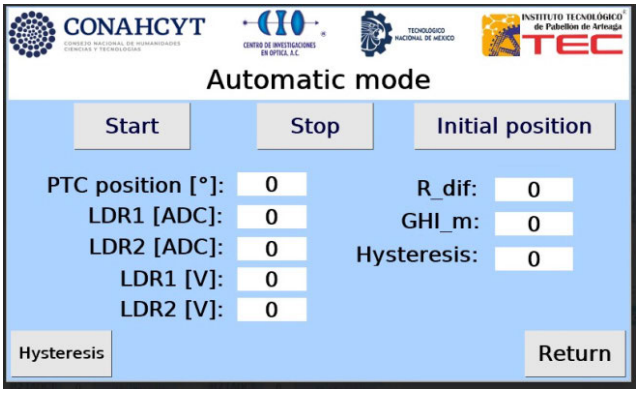

FIGURE 12. Solar tracking monitoring and control system interface: automatic mode screen.

In addition, Table 3 describes the approximate costs of the modular electronics, interface elements, and other materials involved in the construction of the solar tracking system, without considering labor costs or other expenses. The approximate total cost of the developed solar tracker was $700.25 USD.

TABLE 3. Approximate cost of the solar tracker.

PIECES	ELEMENT	COST (USD)
1	Solar sensor: LDR with base.	$3.25
1	Raspberry Pi 3B 2GB RAM w/5V 3A power supply.	$163.85
1	Arduino Mega 2560 w/5V 1A power supply.	$26.96
1	NX8048T070 7"- HMI-screen touch.	$138.89
1	Stepper motor driver TB6600 5A 42V.	$23.39
2	3.3V 5V USB to TTL CH340G module adapter.	$5.00
2	Limit switch ME-8108.	$11.66
1	Kit of powers supply 100-240V AC and short circuit protection elements (relay, switches, power supply units).	$147.26
1	Kit of Panel, 3D supports, connection elements, electrical wiring and terminals, selector, pilot light.	$179.99
	Total	$700.25

III. RESULTS

A. INTEGRATION OF THE PROPOSED HYBRID EXTRUDER MACHINE

The assembly and final integration of the PTC with the solar tracking system in the hybrid extruder machine was carried out, as shown in Figure 13. The operation of the electrical resistances and the operation of the PTC with solar tracking was verified before to carry out the thermal experimentation tests. The solar tracking movement system provides stability and rotation control to the parabolic collector, managing to orient the position of the PTC in such a way that most of the solar radiation is concentrated in the receiver (barrel) of the parabola, which it absorbs heat and increases its temperature.

B. EXPERIMENTAL RESULTS

1) EXPERIMENTAL SETUP

For comparative purposes, in the present experimental campaign, three heating configurations of the proposed extruder were performed: (1) through electrical resistances, (2) through solar radiation, and (3) through a hybrid system (resistances plus solar energy).

The experimentation was carried out at the Instituto Tecnológico de Pabellón de Arteaga, Pabellón de Arteaga, Aguascalientes, México, located at a longitude of 102° 16' 8.04'' W and latitude 22° 09' 42.11'' N. With the support of a brand thermographic camera Flir E5-XT, the temperature reached by the barrel (receiver) and the times to reach the stable state of the temperature were measured, which was established at 200 ±15 °C as the desired reference for all the experiments, with a lower limit set at 185 °C and an upper limit at 215 °C.

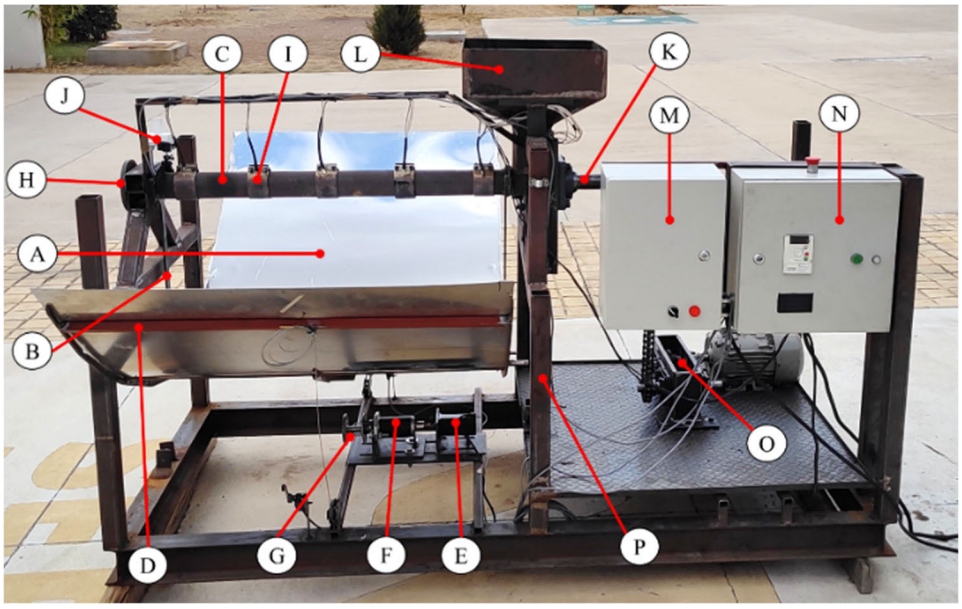

FIGURE 13. Hybrid extrusion machine built: A) PTC, B) floating vertical supports, C) barrel (receiver), D) frame, E) gear motor, F) DC motor, G) winch system, H) extruder nozzle, I) electrical resistances, J) solar sensor, K) screw, L) feeding hopper, M) solar tracking panel, N) 220V electrical control panel, O) power transmission equipment (AC motor, gearbox, chain), and P) support structure.

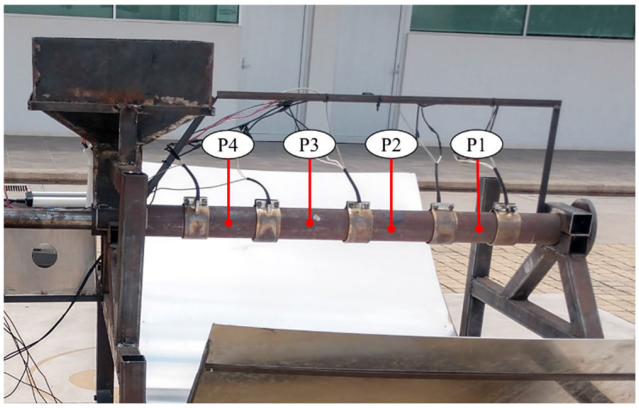

FIGURE 14. Temperature measurement points on the receiver of the extruder machine: P1, P2, P3, and P4.

In each experiment, the same thermal monitoring points (P1, P2, P3, P4) on the receiver were considered, see Figure 14. According to the experimental heating configuration, heating times of 2, 3 or 5 hours were established. The heating time of the barrel using solar energy can be relatively long compared to electric resistances. However, it is important to mention that the system used in the experimentation is a functional prototype that was used to conduct a proof of concept in an actual environment. Using a bigger collector to attain a higher solar concentration level would be sufficient to reduce the heating time.

During the test days, the level of solar radiation (W/m^2), the wind speed (km/h) and the electrical energy consumption (kWh) of the electrical resistances were recorded. DNI data were obtained from the automatic weather station located at the Aguascalientes meteorological observatory, located at longitude 102° 17' 28.28'' W and latitude 21° 51' 03.39'' N (belonging to the National Meteorological Service (Mex.) available in [36]).

An RZ GM816 digital anemometer was used for measure wind speed and the PZEM 022 current meter was used for energy consumption. It is worth mentioning that the thermal characterization of the system was carried out without the extrusion of material so as not to affect the results and to be able to make an equitable comparison of the thermal performance between the defined experimental models.

2) HEATING BY ELECTRICAL RESISTANCES

For the experimental tests of heating by electric resistances, the solar tracking of the PTC was not activated. The extruder machine was placed under an architectural roof in order to carry out the experiments under shade; however, it was exposed to the presence of gusts of wind. The tests were performed during the periods from October 25 to November 16, 2022 and from March 16 to April 12, 2023. The resistors were attached to the body of the barrel and put into operation. For these tests, a maximum time of 2 hours of operation of the resistors was established from 11:00 to 13:00 h (local time).

Figures 15 and 16 shows the experimental results of the typical heating obtained through electrical resistances on the days of November 9, 2022 and April 3, 2023, respectively. On both days, a similar behavior was observed: (1) a low level of wind speed (less than 7 km/h); (2) the initial temperature of the receiver was 19.4 and 28.5 °C (room tempera-

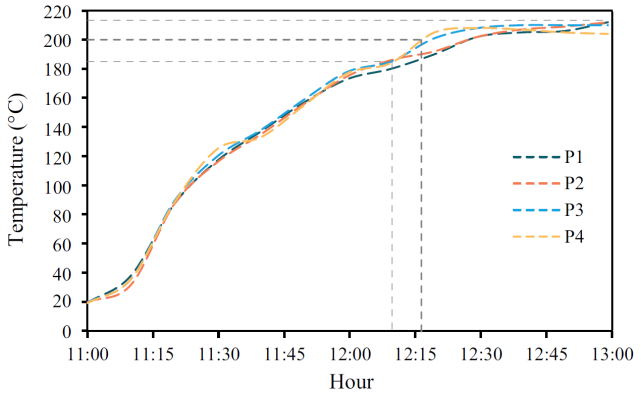

FIGURE 15. Temperatures reached in the receiver through the resistances on November 9, 2022.

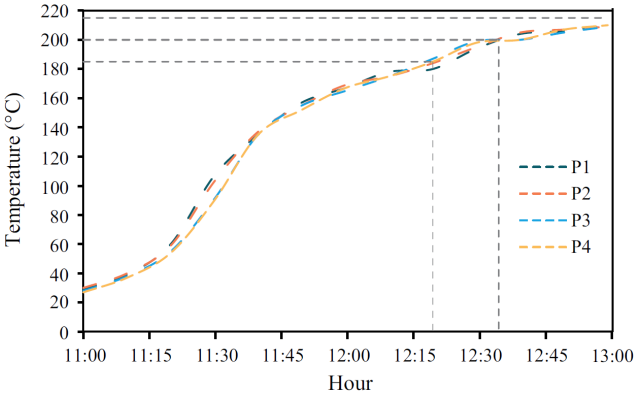

FIGURE 16. Temperatures reached in the receiver through the resistances on April 3, 2023.

ture), respectively; (3) the resistors, upon being turned on, rapidly heat the receiver until reaching thermal stability within the desired heating range; (4) for the days presented, 185 °C was reached between 70 and 80 minutes of operation, while 200 °C was reached at 77 and 95 minutes of ignition; (5) the difference in times observed to reach temperatures of 185 and 200 °C between the days presented is mainly due to the natural decrease in the efficiency (useful life) of the resistors, a disadvantage observed in this type of heating system, and (6) during the time of the experimentation, the temperature of 215 °C was never exceeded; however, it can be inferred that if the heating had continued, this level would have been surpassed.

In the same way, during the days of experimentation, the measurement of the current consumption of the resistor arrangement was conducted. On November 9, 2022, an approximate energy consumption of 2.3 and 2.55 kWh was recorded to reach temperatures of 185 and 200 °C, respectively. Similarly, on April 3, 2023, the values of 185 and 200 °C were reached with an electrical consumption of 2.65 and 3.15 kWh. It is worth mentioning that these consumption values only consider the 2 hours of operation of the resistors.

3) HEATING BY THE PTC SYSTEM WITH SOLAR TRACKING

The heating experiments by the PTC system with solar tracking were carried out outdoors in a sunny area and were performed in the periods from September 30 to October 28, 2022 and from April 12 to May 15, 2023 on a regular schedule. from 11:00 to 14:00 h (local time). In this case, solar tracking allowed DNI to be concentrated on the extruder barrel without the effect of electrical resistances. The graphs obtained in two days of solar tracking with a clear day and with a wind speed of less than 7 km/h are presented.

Figures 17 and 18 shows, respectively, the temperatures reached by the receiver on October 27, 2022 and May 11, 2023. In general, on both days an increase in the receiver temperature can be seen as the time of solar concentration advances. The maximum temperature reached at point P4 of the receiver, on October 27, 2022, was 96 °C, with the average initial temperature of the receiver being 22 °C. However, the temperature of point P1 only reached a temperature of 56 °C due to the geometric losses caused by the end of the collector, which will be analyzed later. The low temperatures reached in the receiver are mainly due to the fact that, on the date the experiment was carried out, the Global Horizontal Irradiance (*GHI*) is low, because it never reaches 1,000 W/m^2. On the other hand, thanks to the high level of *GHI* presented on

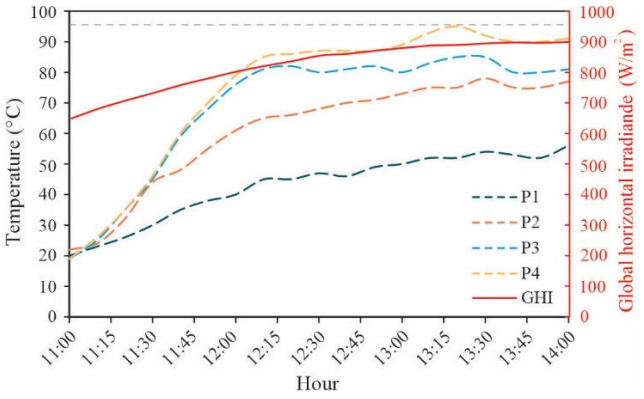

FIGURE 17. Temperatures reached in the receiver through the PTC on October 27, 2022.

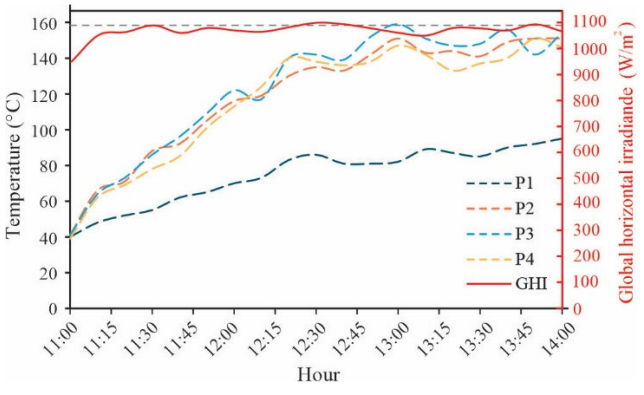

FIGURE 18. Temperatures reached in the receiver through the PTC on May 11, 2023.

May 11, 2023 (radiation greater than 1,000 W/m^2), a wide temperature gradient was obtained, starting at 40 °C and reaching a maximum of 159 °C (see Fig. 18). It is important to mention that the initial temperature of the receiver on this day was not equal to the ambient temperature because the receiver received solar radiation before starting the test, increasing its temperature.

As observed, on both days of experimentation it was not possible to reach the desired temperature (200 ±15 °C) only with the solar radiation concentrated by the PTC; however, it is found that this configuration can be used to preheat the receiver or as auxiliary support for electrical resistances in a hybrid heating system.

As is well known, PTCs are typically exposed to collector end geometry losses. Figure 19 shows how these losses were present in the experimentation on October 27, 2022 and May 11, 2023, where a shading is observed at point P1, which means that it did not receive constant radiation at throughout the day, considerably affecting the temperature of this point since it did not even reach 100 °C (see Fig. 18). The degree of geometric losses generally varies according to the date of the experimentation and the latitude of the place. Regularly, the percentage of losses is usually reduced by increasing the length of the collector.

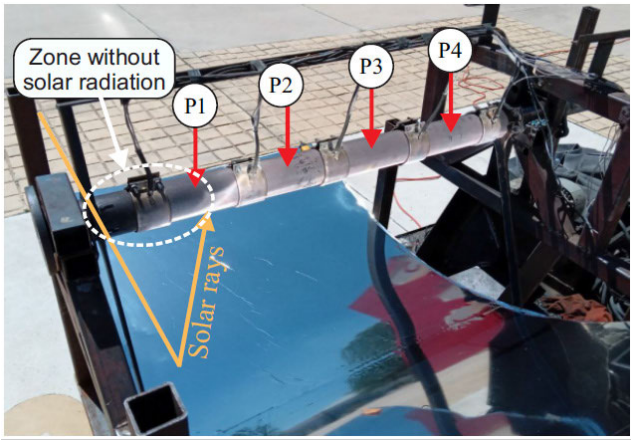

FIGURE 19. Geometric losses due to the end of the collector on point P1 (May 11, 2023).

4) HEATING BY THE HYBRID SYSTEM

The hybrid heating model of the proposed extruder is based on the operation of the PTC with solar tracking plus electrical resistances. There are two modes in which the system can be executed: (a) hybrid mode with preheating: the PTC is used as an initial preheating system and after a period of time the resistors are activated to reach the desired extrusion temperature, and (b) total hybrid mode: the PTC and the electrical resistances are activated from the beginning of operation to reach the desired temperature more quickly.

The heating tests by the hybrid system were carried out outdoors in a sunny area and were performed in the periods from October 25 to November 16, 2022 and from May 15 to 31, 2023 at 11:00 to 16:00 h (local time). The graphs obtained in days of hybrid operation are presented during clear days and with wind speed less than 7 km/h.

a: HYBRID MODE WITH WARM-UP

During the present experimentation, firstly, the PTC with solar tracking was put into operation exclusively for a period of 180 min (from 11:00 to 14:00 h local time); After this time, the electrical resistances were activated for 120 min (from 14:00 to 16:00 h local time). Figure 20 presents the temperatures reached in the receiver (barrel) on November 10, 2022, a season of the year in which solar radiation is not high (*GHI* < 1000 W/m^2 throughout the day). In this case, the preheat reached a temperature of up to 79 °C at point P4 after 180 min (orange area of Fig. 20); then, the electrical resistances were activated and the hybrid system took approximately 41 min to reach 185 °C, and 57 min to reach a temperature of 200 °C, that is, 41.4 and 25.97% less time than required for exclusive heating with electric resistance. Note that, immediately when hybrid mode is entered (green zone in Fig. 20), there is a step in the temperature increase at all points in the receiver. Likewise, it is important to note that 215 °C was reached in approximately 81 min, something not achieved in 120 min of heating with electrical resistances (see Section III-B.2).

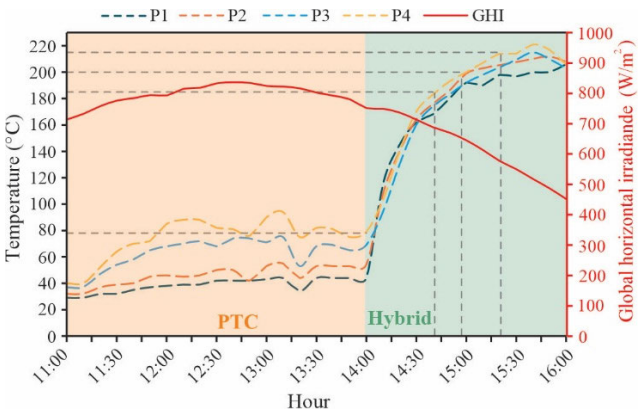

FIGURE 20. Temperatures reached in the hybrid mode with preheating on November 10, 2022.

Similarly, Figure 21 shows the behavior of the temperatures in the receiver on May 30, 2023, a day with a high level of *GHI*. On this day, a temperature of 147 °C was reached during preheating (only with the PTC, see orange zone), and just 18 min after activating the electrical resistances, a maximum temperature of 185 °C was recorded at one point in the receiver, and 25 min to reach 200 °C, a reduction of 77.50 and 73.68% of the time used by the electrical resistances, respectively. The receiver reached a maximum of 215 °C in just 49 min. In the same way as in the case of exclusive heating by the PTC, point P1 was affected by the losses at the end of the collector on the days analyzed; however, when the system works in its hybrid mode, the resistors compensate for this problem, managing to increase the temperature of said point

TABLE 4. Comparative summary of the experimentation.

METHODOLOGY	DATE	Times (min) to reach the temperatures (°C) of:			Electrical consumption (kWh) to reach the temperatures (°C) of:			Decreased consumption to reach 200 °C
		185	200	215	185	200	215	
Resistances	09/11/2022	70	77	≈120	2.30	2.55*	3.90	
Hybrid mode with warm-up	10/11/2022	41	57	81	1.35	1.89	2.63	25.97%
Resistances	03/04/2023	80	95	≈129	2.65	3.15**	3.90	
Hybrid mode with warm-up	30/05/2023	18	25	49	0.60	0.83	1.48	73.68%
Full hybrid mode	31/05/2023	27	30	43	0.89	0.99	1.30	68.42%

* Value used as a reference for comparison with November 10, 2022.
** Value used as a reference for comparison with May 30 and 31, 2023.

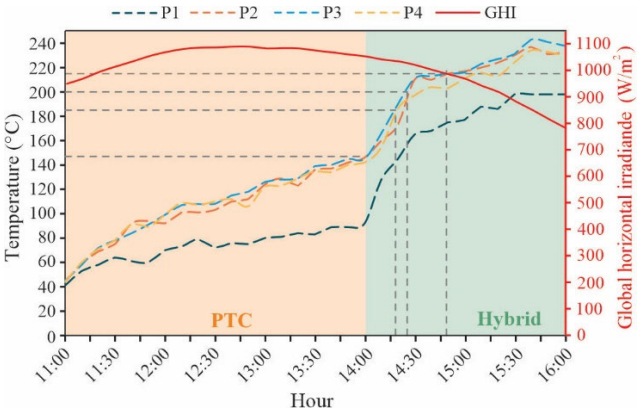

FIGURE 21. Temperatures reached in hybrid mode with preheating on May 30, 2023.

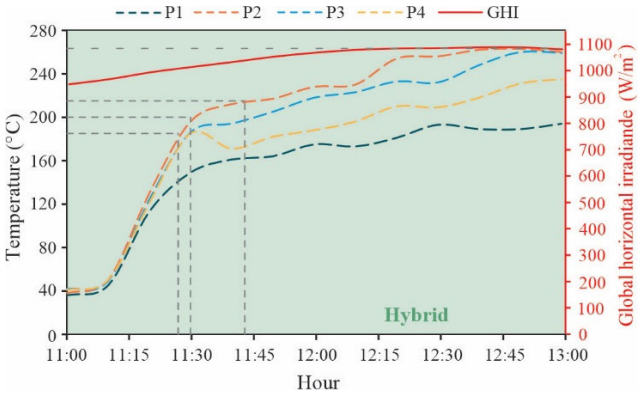

FIGURE 22. Temperatures reached in the total hybrid tests of PTC + resistance at the same time on May 31, 2023.

above 185 °C. The experimental results showed a significant reduction in the operation time of the electrical resistances to reach the desired temperatures and, consequently, there would be a decrease in the costs of energy expenditure, which suggests that the integration of solar energy within a process extrusion is feasible.

b: FULL HYBRID MODE

Additionally, the behavior of the total hybrid system was analyzed, activating simultaneously from the beginning the electrical resistances and the PTC with solar tracking.

Figure 22 shows the results of May 31, 2023, under this heating mode. Starting from an initial temperature of 39 °C (receiver exposed to the elements prior to the tests), times of 27, 30, and 43 min were recorded to reach 185, 200 and 215 °C, respectively. Comparing these results against those obtained by the exclusive use of electrical resistances (see Fig. 16), a decrease of 66.25 and 68.42% was achieved in the operation times of the resistances to reach temperatures of 185 and 200 °C, respectively.

As can be seen, if a high receiver temperature in a minimum time is desirable, this heating mode could be the best option, since temperatures higher than 260 °C were reached, something not achieved in the other modes of heating. Otherwise, if it is desired to keep the temperature within the range of 200 ±15°C, it would be possible to instantly turn off the resistances, which would allow a greater saving of electrical energy during extrusion.

Finally, Table 4 summarizes the most important results obtained in the experimentation. Considering the base temperature of 200 °C: (a) in the hybrid mode with preheating, the extruder receiver reaches the desired temperature faster and with less electrical consumption than with the exclusive use of electrical resistances, allowing a savings of 25.97 and 73.68% for the days of November 10, 2022 and May 30, 2023, respectively; and (b) similarly, in the full hybrid mode, an energy saving of 68.42% was observed for May 31, 2023, which was similar to that obtained in the hybrid experimentation with heating on May 30, 2023 (day with a similar level of radiation), so it can be concluded that both hybrid modes produce a similar result of energy savings. It is important to mention that the savings percentages may vary depending on the level of the *GHI*, wind speed and ambient temperature.

IV. CONCLUSION

This paper presents the design and construction of a hybrid horizontal extruder machine (electric and solar), which uses a parabolic trough system with solar tracking to concentrate direct normal irradiation in a linear focus, where it is located. the extruder barrel (receiver).

For this, the design and the optical simulation were preformed to determine the optimal geometry of the collector and receiver of the PTC, reaching an average solar concentration of 3.85x; that is to say, 3,850 W/m^2. With this simulation, the solar tracking tolerance of $\pm 4.2°$ was estimated, which ensures that the optical efficiency remains above 98%. This wide tolerance allowed the solar tracker to avoid the need to continuously update its position, having lower power consumption during solar tracking. The integration of the proposed extruder machine with the parabolic trough system with solar tracking is presented.

For comparative purposes and validation of the operation in a real environment, experimental heating tests of the extruder barrel were performed following the three methods: (1) electrical resistances, (2) PTC with solar tracking (solar radiation), and (3) hybrid with preheating and total hybrid. Likewise, tests were carried out in two different seasons of the year to compare the impact of the level of solar radiation on the system.

The times in which at least one point of the receiver reached the desired temperature of 200 $\pm$15 °C were measured and the following was concluded:

(a) Heating by means of electrical resistances allowed us to validate that said arrangement is capable of reaching the desired temperature (200 °C), it was observed that approximately between 77 and 95 min are required to reach this objective.

(b) In the case of the exclusive use of heating with PTC (solar radiation), maximum temperatures of up to 159 °C were recorded and, despite the fact that the desired temperature was not reached, it is evident that this mode can be used as system of pre-heating or complement of the electrical resistances, which helps to reduce the operating times of the resistances.

(c) The hybrid mode with preheating allowed a time reduction between 25.97 and 73.68% to reach 200 °C in the receiver with respect to the times presented with electrical resistances. Variations over time depended mainly on the *GHI*level on the testing day. In addition, a maximum temperature of 243 °C was reached in a period of two hours from the activation of the electrical resistances.

(d) In full hybrid heating, the time needed to reach 200 °C was reduced by 68.42% compared to that required by electrical resistances, and an approximate maximum temperature of 260 °C was reached in the receiver after two hours of operation, being the highest temperature recorded in all heating modes. Since this temperature already drastically exceeds the target temperature, it would be possible to instantly turn off the resistors in the extrusion process, allowing for further electrical energy savings.

As previously mentioned, the proposed extruder machine is just a prototype created for research, reaching temperatures up to 260 °C. However, it is possible to increase the solar concentration and temperature level of the barrel by increasing the length or opening of the parabolic trough collector and the heating time could be reduced using a bigger collector too. The general results allowed us to analyze the feasibility of integrating the use of solar radiation to carry out an extrusion process. In particular, the proposed prototype can be classified as a medium-temperature solar concentration device, as the temperature reached are suitable for extruding plastics like polystyrene, polypropylene and polyethylene.

As future work, it is intended to carry out the actual extrusion of material to include an economic analysis of the prototype and to optimize the design and configuration of the system.

ACKNOWLEDGMENT

The authors would like to thank Raúl Llamas Esparza and Juan Manuel Bernal Medina for their technical assistance in the development of the project and also would like to thank the company Micro Refinería Ecológica S. de R. L. de C. V. for the technical advice provided.

REFERENCES

[1] A. Adisa, O. Olatunji, and K. Brando, "Design of extrusion machine for offshore corrosion-control composite wrap material manufacture," in *Proc. SPE Nigeria Annu. Int. Conf. Exhib.*, 2020, doi: 10.2118/203729-MS.

[2] H. Li et al., "Expanding plastics recycling technologies: Chemical aspects, technology status and challenges," *Green Chem.*, vol. 24, no. 23, pp. 8899–9002, Nov. 2022, doi: 10.1039/d2gc02588d.

[3] Herianto, S. I. Atsani, and H. Mastrisiswadi, "Recycled polypropylene filament for 3D printer: Extrusion process parameter optimization," *IOP Conf. Ser., Mater. Sci. Eng.*, vol. 722, no. 1, Jan. 2020, Art. no. 012022, doi: 10.1088/1757-899X/722/1/012022.

[4] S. Kumar, R. Sooraj, and M. V. V. Kumar, "Design and fabrication of extrusion machine for recycling plastics," *IOP Conf. Ser., Mater. Sci. Eng.*, vol. 1065, no. 1, Feb. 2021, Art. no. 012014, doi: 10.1088/1757-899X/1065/1/012014.

[5] M. L. Sonjaya and M. F. Hidayat, "Construction and analysis of plastic extruder machine for polyethylene plastic waste," *EPI Int. J. Eng.*, vol. 3, no. 2, pp. 132–137, Jan. 2021, doi: 10.25042/epi-ije.082020.07.

[6] R. A. García-León, A. Bohorquez-Niño, and J. F. Barbosa-Paredes, "Design of an extrusion machine for the manufacture of plastic tubes," *J. Phys., Conf. Ser.*, vol. 1257, no. 1, Jun. 2019, Art. no. 012006, doi: 10.1088/1742-6596/1257/1/012006.

[7] C. Budiyantoro, H. S. B. Rochardjo, and G. Nugroho, "Design, manufacture, and performance testing of extrusion–pultrusion machine for fiber-reinforced thermoplastic pellet production," *Machines*, vol. 9, no. 2, p. 42, Feb. 2021, doi: 10.3390/machines9020042.

[8] H. Brito, C. Flores, and K. G. Salazar-Llangari, "Diseño y construcción de un extrusor tipo tornillo para la obtención de pellets plástico a partir de botellas recicladas," in *Proc. 36th Congreso Interamericano de Ingeniería Sanitaria y Ambiental*, Oct. 2018.

[9] S. Mekhilef, R. Saidur, and A. Safari, "A review on solar energy use in industries," *Renew. Sustain. Energy Rev.*, vol. 15, no. 4, pp. 1777–1790, May 2011, doi: 10.1016/j.rser.2010.12.018.

[10] "IEA-ETSAP, IRENA, solar heat for industrial processes—Technology brief," Tech. Rep., 2015. [Online]. Available: https://www.irena.org

[11] A. Modi, F. Bühler, J. G. Andreasen, and F. Haglind, "A review of solar energy based heat and power generation systems," *Renew. Sustain. Energy Rev.*, vol. 67, pp. 1047–1064, Jan. 2017, doi: 10.1016/j.rser.2016.09.075.

[12] E. Kabir, P. Kumar, S. Kumar, A. A. Adelodun, and K.-H. Kim, "Solar energy: Potential and future prospects," *Renew. Sustain. Energy Rev.*, vol. 82, pp. 894–900, Feb. 2018, doi: 10.1016/j.rser.2017.09.094.
[13] N. M. Sheikh, "Efficient utilization of solar energy for domestic applications," in *Proc. 2nd Int. Conf. Electr. Eng.*, Lahore, Pakistan, Mar. 2008, pp. 1–3, doi: 10.1109/ICEE.2008.4553911.
[14] B. Boutaghriout, A. Bouakaz, C. Hamouda, H. Smadi, and A. Malek, "Investigation on the use of solar thermal energy in the agro food industry in Algeria," in *Proc. Int. Renew. Sustain. Energy Conf. (IRSEC)*, Ouarzazate, Morocco, Mar. 2013, pp. 167–170, doi: 10.1109/IRSEC.2013.6529716.
[15] M. I. Mohammed, D. Wilson, E. Gomez-Kervin, L. Rosson, and J. Long, "EcoPrinting: Investigation of solar powered plastic recycling and additive manufacturing for enhanced waste management and sustainable manufacturing," in *Proc. IEEE Conf. Technol. Sustainability (SusTech)*, Long Beach, CA, USA, Nov. 2018, pp. 1–6, doi: 10.1109/SusTech.2018.8671370.
[16] J. N. González, A. B. Morales, M. R. Corona, and J. V. Munguía, "Numerical simulation of a polymer melting process using solar energy," *Suplemento de la Revista Mexicana de Física*, vol. 1, no. 2, pp. 18–24, Jul. 2020.
[17] E. Zarza, "Medium temperature solar concentrators (parabolic-troughs collectors)," *Sol. Energy Convers. Photoenergy Syst.*, vol. 1, no. 8, p. 170, 2009.
[18] A. Kumar, M. Sharma, P. Thakur, V. K. Thakur, S. S. Rahatekar, and R. Kumar, "A review on exergy analysis of solar parabolic collectors," *Sol. Energy*, vol. 197, pp. 411–432, Feb. 2020, doi: 10.1016/j.solener.2020.01.025.
[19] M. Jradi and S. Riffat, "Medium temperature concentrators for solar thermal applications," *Int. J. Low-Carbon Technol.*, vol. 9, no. 3, pp. 214–224, Sep. 2014, doi: 10.1093/ijlct/cts068.
[20] H. Tazvinga, M. Thopil, P.-B. Numbi, and T. Adefarati, "Distributed renewable energy technologies," in *Handbook of Distributed Generation: Electric Power Technologies, Economics and Environmental Impacts*, R. Bansal, Ed. Springer, 2017, pp. 3–67, doi: 10.1007/978-3-319-51343-0.
[21] S. Kannaiyan, N. D. Bokde, and Z. W. Geem, "Solar collectors modeling and controller design for solar thermal power plant," *IEEE Access*, vol. 8, pp. 81425–81446, 2020, doi: 10.1109/ACCESS.2020.2989003.
[22] D. K. De and O. C. Olukunle, "A brief review of solar concentrators," in *Proc. Int. Conf. Energy Econ. Environ. (ICEEE)*, Mar. 2015, pp. 1–7, doi: 10.1109/energyeconomics.2015.7235082.
[23] N. B. Desai and S. Bandyopadhyay, "Line-focusing concentrating solar collector-based power plants: A review," *Clean Technol. Environ. Policy*, vol. 19, no. 1, pp. 9–35, Jan. 2017, doi: 10.1007/s10098-016-1238-4.
[24] T. Q. Saldivar-Aguilera, A. Díaz-Ponce, L. M. Valentín-Coronado, M. I. Peña-Cruz, and G. A. Acevedo-R., "Dual feedback closed-loop control for one-axis solar trackers of parabolic trough collector systems," in *Proc. IEEE Int. Autumn Meeting Power, Electron. Comput. (ROPEC)*, vol. 5, Nov. 2021, pp. 1–6, doi: 10.1109/ROPEC53248.2021.9668095.
[25] C. Xu, M. Li, X. Ji, and F. Chen, "Study on the collection efficiency of parabolic trough solar collector," in *Proc. Int. Conf. Mater. Renew. Energy Environ.*, vol. 1, Aug. 2013, pp. 1–7, doi: 10.1109/icmree.2013.6893602.
[26] H. A. K Shahad, S. H. Hammad, and N. A. Ghyadh, "Design, fabrication and performance testing of PTC with helical coil receiver," in *Proc. 4th Sci. Int. Conf. Najaf (SICN)*, Apr. 2019, pp. 189–194, doi: 10.1109/SICN47020.2019.9019342.
[27] K. S. Reddy and C. Ananthsornaraj, "Design, development and performance investigation of solar parabolic trough collector for large-scale solar power plants," *Renew. Energy*, vol. 146, pp. 1943–1957, Feb. 2020, doi: 10.1016/j.renene.2019.07.158.
[28] V. K. Jebasingh and G. M. J. Herbert, "A review of solar parabolic trough collector," *Renew. Sustain. Energy Rev.*, vol. 54, pp. 1085–1091, Feb. 2016, doi: 10.1016/j.rser.2015.10.043.
[29] B. Alhayek, M. Agelin-Chaab, and B. Reddy, "Analysis of an innovative direct steam generation-based parabolic trough collector plant hybridized with a biomass boiler," *Int. J. Energy Res.*, vol. 41, no. 14, pp. 1–12, 2017, doi: 10.1002/er.3785.
[30] A. K. Thakur, R. Sathyamurthy, R. Velraj, I. Lynch, R. Saidur, A. K. Pandey, S. W. Sharshir, Z. Ma, P. GaneshKumar, and A. E. Kabeel, "Sea-water desalination using a desalting unit integrated with a parabolic trough collector and activated carbon pellets as energy storage medium," *Desalination*, vol. 516, Nov. 2021, Art. no. 115217, doi: 10.1016/j.desal.2021.115217.
[31] M. Angulo-Calderón, I. Salgado-Tránsito, I. Trejo-Zúñiga, C. Paredes-Orta, S. Kesthkar, and A. Díaz-Ponce, "Development and accuracy assessment of a high-precision dual-axis pre-commercial solar tracker for concentrating photovoltaic modules," *Appl. Sci.*, vol. 12, no. 5, p. 2625, Mar. 2022, doi: 10.3390/app12052625.
[32] D. V. Rosato, *Extruding Plastics: A Practical Processing Handbook*. Dordrecht, The Netherlands: Springer,1998, doi: 10.1007/978-1-4615-5793-7.
[33] S. L. Kumar and H. Vasudevan, "Optimization of injection moulding process parameters the moulding of low density polyethylene (LDPE)," *Int. J. Eng. Res. Devel.*, vol. 7, no. 5, pp. 35–39, 2013.
[34] Imtech Design Ltd. *LDPE Materials*. [Online]. Available: http://www.imtechdesign.com/advice_materials_pe_ld.php
[35] B. J. Huang and S. W. Hsieh, "An automation of collector testing and modification of ANSI/ASHRAE 93-1996 estándar," Tech. Rep., 1990.
[36] Servicio Meteorológico Nacional. *Servicio Meteorológico Nacional*. Accessed: Jul. 19, 2023. [Online]. Available: https://smn.conagua.gob.mx/es/

JOSÉ ALONSO DENA-AGUILAR (Member, IEEE) received the B.S. and M.S. degrees in chemical engineering from Instituto Tecnológico de Aguascalientes, Tecnológico Nacional de México Campus, in 2000 and 2007, respectively, and the Ph.D. degree in biological science from Universidad Autonoma de Aguascalientes, in 2011.

From 2000 to 2005, he participated as the quality manager in different companies. Since 2015, he has been a Professor/Researcher with the Engineering Department, Instituto Tecnológico de Pabellón de Arteaga (ITPA), Tecnológico Nacional de México Campus. He has been the Coordinator of the Division of Graduate Studies and Research, ITPA, since 2018. He is currently acknowledged as a PRODEP profile and realize a postdoctoral stay with Centro de Investigaciones en Óptica, A. C. Campus Aguascalientes, Mexico. His current research interests include technology development and technology transfer related to the application of mechatronics in energy conversion, polymer synthesis, and modeling through artificial intelligence, such as artificial neural networks.

Dr. Dena-Aguilar is a member of the National System of Researchers Level 1 of CONAHCYT and the Founder of the Energy Conversion Laboratory, ITPA.

ARTURO DÍAZ-PONCE received the bachelor's degree in electronic engineering and the M.Sc. degree in electrical engineering from Instituto Tecnológico de Aguascalientes, Tecnológico Nacional de México Campus, and the Ph.D. degree in automatic control from Centro de Investigación y de Estudios Avanzados del Instituto Politécnico Nacional.

In addition, he conducted a research stay with Centro de Domótica Integral, Universidad Politécnica de Madrid. He is currently a CONAHCYT Research Fellow with Grupo de Investigación e Ingeniería en Energía Solar, Centro de Investigaciones en Óptica, A.C., Unidad Aguascalientes. He has worked on issues related to high concentration photovoltaic systems, one or dual axis solar tracking, low-cost solar sensors, solar tracking algorithms, and control systems.

JUAN CARLOS DELGADO-FLORES received the B.S. degree in mechatronics engineering from Instituto Tecnológico de Pabellón de Arteaga (ITPA), Tecnológico Nacional de México Campus, in 2020. He is currently pursuing the Master of Science degree in mechatronic engineering with ITPA.

His B.Sc. thesis "Design and Construction of a Cartesian Robot." His current research interests include mechanical and electronical designs, CNC manufacturing oriented to energy conversion processes, and programming as the Internet of Things.

ERNESTO OLVERA-GONZÁLEZ received the degree in engineering, the master's degree in automatic control from Universidad Autónoma de Querétaro, the Ph.D. degree in engineering science, and the Postdoctoral degree in applied physics from Universidad Autónoma de Zacatecas.

He is currently a Professor/Researcher with Instituto Tecnológico de Pabellón de Arteaga, Tecnológico Nacional de México Campus, and the Founder of the Artificial Illumination Laboratory (LIA), ITPA.

Dr. Olvera-González is a member of the National System of Researchers Level 1 of CONAHCYT. He has had five research projects funded by CONAHCYT and PRODEP. He is also an Accredited Evaluator Member of CONAHCYT (RCEA) of Calls: Technological Innovation Fund (FIT), Innovation Stimulus Program (PEI), and Scientific and Technological Infrastructure.

NIVIA ESCALANTE-GARCÍA received the bachelor's degree in computer engineering, the master's degree in engineering, and the Ph.D. degree in engineering science from Universidad Autónoma de Zacatecas, in 2005, 2011, and 2013, respectively.

She is currently a professor/researcher. She has the recognition of the National System of Researchers (Level 1). She is also the Founder of the Artificial Illumination Laboratory (LIA), Instituto Tecnológico de Pabellón de Arteaga, Tecnológico Nacional de México Campus. She has participated in national and international congresses and has published articles indexed by the Journal Citation Report (JCR). In addition, she has the appointment of accredited evaluator by CONAHCYT (RCA). Her research interests include optical metrology, artificial intelligence, UV-Vis and IR spectroscopy, and artificial radiation focused on food production for human consumption.

VÍCTOR MANUEL VELASCO-GALLARDO received the B.S. degree in electronic engineering and the M.S. degree in industrial engineering from Instituto Tecnológico de Aguascalientes, Tecnológico Nacional de México Campus, in 2006.

From 1998 to 2002, he worked in automotive supplies companies like a process engineer. Since 2003, he has been a professor at different universities. He is currently a Professor/Researcher with the Mechatronic Engineering Department, Instituto Tecnológico de Pabellón de Arteaga (ITPA), Tecnologico Nacional de México Campus. His research interests include the automation of agricultural process, especially in processes that involve the harvest, selection, and packing.

Prof. Velasco-Gallardo won the second place in the contest "Lectura de la Ciencia para Todos," in 2008. He is also acknowledged as a PRODEP profile.